Acknowledgements. We thank members of the Winoto, Allison, Robey and Raulet groups for discussions; P. Schow for technical assistance; A. Nagy, R. Nagy and W. Abramow-Newerly for the R1 ES cells; R. Jaenisch for the J1 ES cells; and E. Robey, B. Ortiz and H. Kasler for critical reading of the manuscript. This work is supported in part by grants from the NIH, National Science foundation and the Keck Foundation. J.Z. was supported by an Irvington Institute fellowship and is a Leukemia Society of America special fellow.

Correspondence and requests for materials should be addressed to A.W. (e-mail: winoto@uclink2.berkeley.edu).

Mutations of mitotic checkpoint genes in human cancers

Daniel P. Cahill*†, Christoph Lengauer*†, Jian Yu*, Gregory J. Riggins*, James K. V. Willson‡, Sanford D. Markowitz‡, Kenneth W. Kinzler* & Bert Vogelstein*

** The Johns Hopkins Oncology Center, Program in Human Genetics, and The Howard Hughes Medical Institute, Johns Hopkins University School of Medicine, 424 North Bond Street, Baltimore, Maryland 21231, USA*

‡Department of Medicine and Ireland Cancer Center, Case Western Reserve University and The Howard Hughes Medical Institute, Cleveland, Ohio 44106, USA

† These authors contributed equally to this study.

Genetic instability was one of the first characteristics to be postulated to underlie neoplasia[1–3]. Such genetic instability occurs in two different forms. In a small fraction of colorectal and some other cancers, defective repair of mismatched bases results in an increased mutation rate at the nucleotide level and consequent widespread microsatellite instability[4–7]. In most colorectal cancers, and probably in many other cancer types, a chromosomal instability (CIN) leading to an abnormal chromosome number (aneuploidy) is observed[8]. The physiological and molecular bases of this pervasive abnormality are unknown. Here we show that CIN is consistently associated with the loss of function of a mitotic checkpoint. Moreover, in some cancers displaying CIN the loss of this checkpoint was associated with the mutational inactivation of a human homologue of the yeast *BUB1* gene; *BUB1* controls mitotic checkpoints and chromosome segregation in yeast. The normal mitotic checkpoints of cells displaying microsatellite instability become defective upon transfer of mutant *hBUB1* alleles from either of two CIN cancers.

The key insight leading to the discovery of the molecular basis of microsatellite instability (MIN) in human tumours was the discovery of a similar phenotype in *Saccharomyces cerevisiae* cells carrying mutations in yeast mismatch repair (MMR) genes[9]. Following this paradigm, we reasoned that the basis for CIN in human tumour cells might be mitotic checkpoint defects similar to those previously observed in yeast cells with chromosomal instability[10–12]. Cells with such defects are expected to exit mitosis prematurely after treatment with microtubule-disrupting agents[12,13]. To test this hypothesis in human colorectal cancer cells, we treated four MIN lines (HCT116, DLD1, RKO, and SW48) and six CIN lines (SW480, HT29, V400, V429, Caco2, and SW837) with nocodazole, a microtubule-disrupting drug. As expected, all lines achieved nearly complete cell-cycle blocks shortly after nocodazole treatment, with DNA contents of 4C (with 2C representing the DNA content in the G1 phase of the cell cycle, before DNA replication has occurred; representative examples are shown in Fig. 1). Morphological analysis of the 4C blocked cells, however, revealed a striking difference between MIN and CIN cells. All MIN cell lines had a normal checkpoint response, resulting in an accumulation of cells with condensed chromosomes characteristic of a sustained mitotic block. In the CIN lines, there was an abnormal response, with many fewer mitotic cells and no clear peak in mitotic index observed at any time point (Fig. 2a). The response of MIN cells was characteristic of those with intact mitotic checkpoints[13], and a similar response was observed in normal human fibroblasts (Fig. 2a).

Consistent differences in mitotic indices were also observed in CIN cells versus MIN cells after treatment with colcemid (Figs 1 and 2b), an agent that blocks microtubules through a different mechanism from that of nocodazole. This defect was further established by the higher fraction of CIN cells that synthesized DNA during nocodazole or colcemid treatment (Fig. 2c). There was little overlap between the responses observed in MIN and CIN cells in these

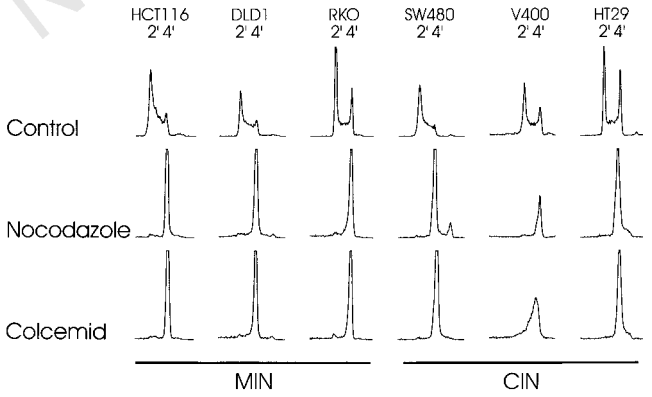

Figure 1 Analysis of the cell cycle of MIN and CIN cells. MIN (HCT116, DLD1, and RKO) and CIN (SW480, V400, and HT29) cells were treated with nocodazole or colcemid for 18 h, stained with Hoechst 33258, a DNA-specific dye, and analysed by flow cytometry. 2′ and 4′ refer to the DNA contents of each cell line in G1 and G2/M phases, respectively.

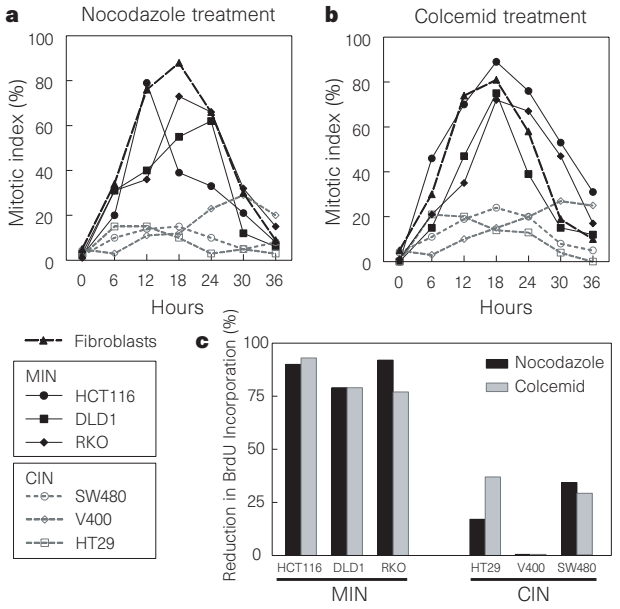

Figure 2 Mitotic indices and DNA synthesis in MIN and CIN cells. Cells were treated with nocodazole (**a**) or colcemid (**b**) for the indicated times, stained with H33258, and analysed by fluorescence microscopy. **c**, BrdU was added to the nocodazole- or colcemid-treated cultures 2.5 h before collection. The bars represent the percentage reduction in BrdU incorporation compared with untreated cells, assessed using an antibody to BrdU. At least 200 cells were counted for each determination and the result shown is representative of those observed in three independent experiments.

assays. For example, the decrease in bromodeoxyuridine (BrdU) incorporation into newly synthesized DNA ranged from 61% to 92% in MIN cells and from 0% to 34% in CIN cells. Similarly, the maximal mitotic indices achieved following 12–18 h of colcemid treatment ranged from 72% to 89% in the four MIN lines, whereas those in the six CIN lines ranged from 20% to 31% ($P < 0.01$ by two-tailed Student's *t*-test).

To elucidate the genetic mechanisms underlying the checkpoint defect in CIN cells, we chose first to evaluate the human homologue of *S. cerevisiae BUB1*. *BUB1* is the prototype member of a family of genes, some of which encode proteins that bind to the kinetochore and all of which are required for a normal mitotic delay in response to spindle disruption[14–17]. The human (h) homologue of *BUB1* was cloned and the complete coding sequence determined using a combination of DNA-database searches and reverse transcription with polymerase chain reaction (RT-PCR) methods. Comparison with the *S. cerevisiae BUB1* gene showed that these two genes contain two highly conserved domains (CD1 and CD2; Fig. 3a). CD1 (*hBUB1* codons 21–152) directs kinetochore localization and binding to Bub3 whereas CD2 (codons 732–1043) encodes the kinase domain[15,18]. We isolated a genomic clone containing the *hBUB1* gene and used it to map the location of *hBUB1* to chromosome 2q12-14 through fluorescence *in situ* hybridization (FISH).

We then selected 19 colorectal cancer cell lines with a CIN phenotype to search for mutations in *hBUB1* through RT-PCR-mediated amplification and direct sequencing of the entire coding region of *hBUB1*. RT-PCR analysis of V400 (one of the lines whose phenotype is shown in Figs 1 and 2) revealed a small amplification product (~800 base pairs (bp)) in addition to one of normal size (~1,000 bp). Sequencing of the shorter RT-PCR product showed that it was the result of an internal deletion of 197 bp, predicted to remove codons 76 to 141 and create a frameshift immediately thereafter. Sequencing of the relevant region of genomic DNA identified a G-to-A transition at the canonical splice donor site, which comprises the first intronic nucleotide following codon 140 (Fig. 3b). Sequence analysis of cDNA from another line, V429, revealed a missense mutation at codon 492 (Fig. 3b) that resulted in the substitution of tyrosine for a conserved serine. In both V400 and V429, the mutations were heterozygous and the second allele of the pair was wild type (WT). Analysis of DNA derived from archived tissues of the patients from whom these cell lines were derived revealed that the mutations were somatic, present in their primary tumours but not in their normal tissues (Fig. 3b).

To determine whether the mutant alleles in V400 and V429 could be functionally distinguished from null or WT alleles, we expressed them in MIN cells and evaluated the cells' behaviour following microtubule disruption. Expression vectors encoding both an *hBUB1* cDNA (either WT or one of the two mutants) and a green fluorescent protein (GFP) gene were constructed and transfected into MIN cell lines. We treated cells with nocodazole and productively transfected cells were isolated by cell sorting on the basis of GFP fluorescence (Fig. 4). Over 90% of transfected cells were found to accumulate a DNA content of 4C following nocodazole treatment, regardless of which *hBUB1* sequences were present in the

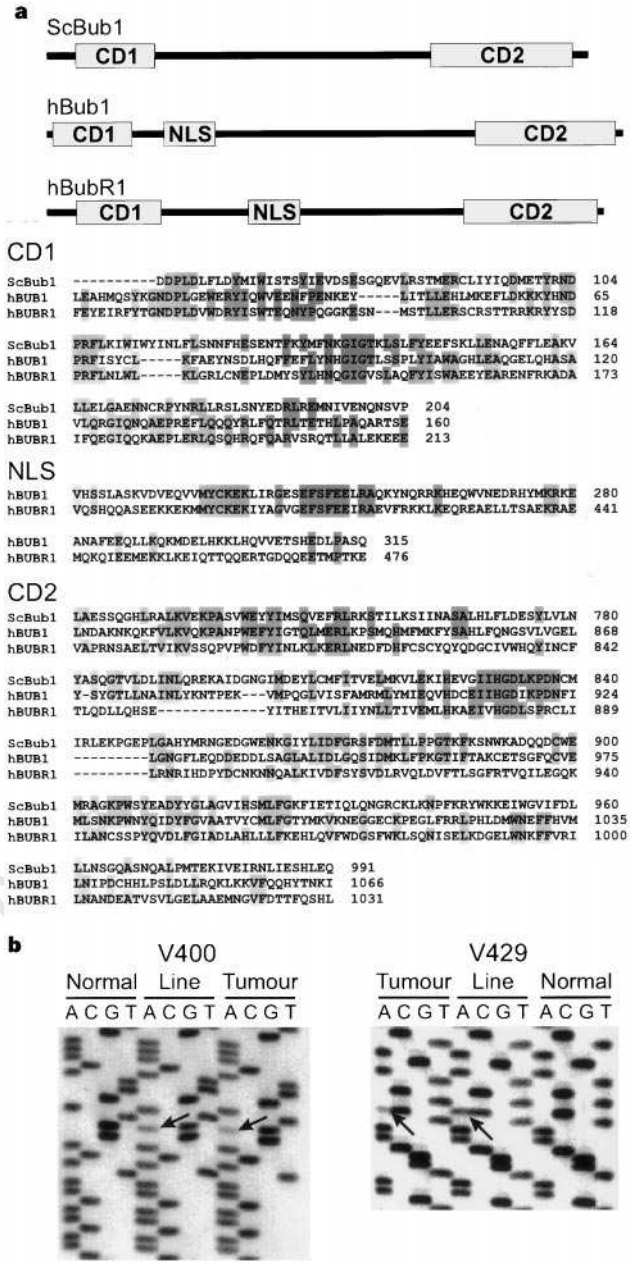

Figure 3 Sequence analysis of human *BUB1* genes. **a**, *S. cerevisiae* (Sc) and human protein sequences were aligned using Macaw Version 2.0.3. CD1, NLS (nuclear-localization signal), and CD2 represent sequence blocks that are highly related among the genes. Identical amino acids are shaded. **b**, Sequence of *hBUB1* in CIN cell lines V400 and V429, in normal cells and in the primary tumours from the patients from whom the corresponding cell lines were derived. Arrows indicate the G-to-A transition at the canonical splice donor site following codon 140 in line V400 and the C-to-A transversion at codon 492 in line V429.

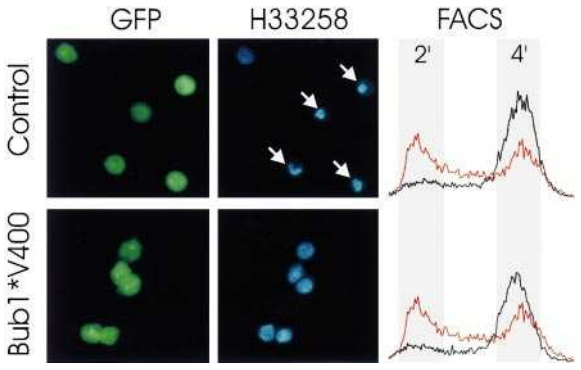

Figure 4 The *hBUB1* expression system. Following transfection of an expression vector encoding mutant *hBUB1* from V400 (Bub1*V400) or of a control vector without *hBUB1*, into HCT116 cells, fluorescence-activated cell sorting (FACS) was used to isolate transfected cells on the basis of GFP expression. Cells were analysed with fluorescence microscopy to ensure that the sorted cells expressed GFP (left panels), and to analyse both mitotic indices following H33258 staining (middle panels) and cell-cycle distributions (right panels). Arrows point to cells in mitosis. The cell-cycle distributions before (red profiles) and after (black profiles) nocodazole treatment are shown on the right. 2′ and 4′ are defined in Fig. 1.

vector (examples in Fig. 4). However, expression of either of the mutant *hBUB1* genes substantially altered the mitotic indices of transfected cells after nocodazole treatment, whereas the WT *hBUB1* gene had little effect, compared with a control vector lacking *hBUB1* sequences (Fig. 5a). These results indicated that both mutants could confer a dominant-negative effect in two different MIN cell lines, at least when overexpressed relative to endogenous levels. To determine whether a dominant-negative effect was observed when mutant and WT genes were expressed at equivalent levels, we performed cotransfections. Both *hBUB1* mutant expression vectors resulted in altered checkpoint status when transfected with an equal amount of the WT *hBUB1* expression vector; the mitotic index was decreased by 45–69% compared with the index resulting from transfection of the WT *hBUB1* expression vector alone.

If the *hBUB1* mutants caused a premature exit from mitosis in the presence of microtubule disruption, one would expect that such cells would re-enter S phase, just as did the CIN cells depicted in Fig. 2c. To address this point, we added BrdU to the culture media of nocodazole-treated, *hBUB1*-transfected HCT116 cells 2.5 h before collecting them. As shown in Fig. 5b, there was significantly less reduction in BrdU incorporation after transfection with either of the two mutant *hBUB1* expression constructs than after transfection with the WT *hBUB1* expression construct or with the control vector. A similar re-entry into S phase was observed in DLD1 cells after expression of mutant *hBUB1* genes (Fig. 5b).

Because many genes control the mitotic checkpoint in yeast, we searched for additional genes that might play a role in this process in humans. Another *BUB1* homologue, named *hBUBR1*, was identified and its sequence determined through a strategy similar to that described above for *hBUB1* (Fig. 3a). The *hBUBR1* gene is of comparable size to *hBUB1* but is less homologous to the murine *BUB1* gene (29% versus 81% identical residues in the conserved domains, respectively). Sequence comparisons also revealed a third domain between CD1 and CD2 that contains a putative nuclear-localization signal that is present in both human homologues and in murine *BUB1* but not in the yeast gene (Fig. 3a). We isolated a bacterial artificial chromosome (BAC) clone containing *hBUBR1* and used it in FISH experiments to show that the gene is located on human chromosome 15q14-21. We found the *hBUBR1* gene, like *hBUB1*, to be expressed in all 19 CIN cancers analysed. Using RT-PCR products as templates for sequencing, we noted several variants of *hBUBR1* that are likely to be polymorphisms on the basis their frequency. We also found two mutations, neither one of which was found among 40 normal alleles. The first was a germline C-to-T transition at codon 40, resulting in a substitution of methionine for threonine, in line V531. The second mutation, found in line V1394, was a somatic deletion of T at codon 1,023. Although this latter mutation would be predicted to remove part of the kinase domain within CD2 (ref. 19), further studies will be required to determine whether either of these *hBUBR1* mutations functionally alters the gene product.

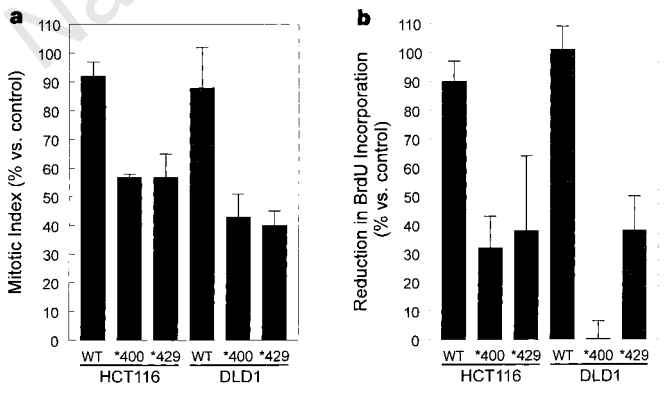

Figure 5 Effects of *hBUB1* expression. Mitotic indices (**a**) or BrdU incorporation (**b**) in nocodazole-treated, *hBUB1*-transfected cells were compared with mitotic indices or BrdU incorporation in control-transfected cells. Transfected cells were isolated through cell sorting on the basis of GFP fluorescence. The shaded bars and error bars represent the means and standard deviations, respectively, determined from at least two independent assessments of 100 cells each in a single experiment; similar results were obtained in two independent experiments. The *hBUB1* expression vectors (WT or mutant from V400 [*400] or V429 [*429]), and the cell lines transfected (HCT116 and DLD1), are indicated.

The results described above indicate that all tested CIN cell lines were defective in a well defined mitotic checkpoint and had a phenotype similar to that seen in yeast cells with genetic alterations of mitotic checkpoint genes such as *BUB1*. Although such results, in addition to the mutational analyses reported above, do not prove that aneuploidy can be due to defects in mitotic checkpoints, the data are consistent with this possibility. This hypothesis is supported by the fact that the expression of either of two naturally occurring *hBUB1* mutants converted the normal checkpoint status of MIN cells to the defective type characteristic of CIN cells. Analogously, it has been shown that expression of *in vitro*-generated variants of murine BUB1 allowed cells to exit mitosis prematurely[18]. Such dominant-negative effects are intriguing in light of the previous demonstration that the CIN phenotype is dominant upon fusion of MIN and CIN cells[8].

It will be important to determine whether defects in other mitotic checkpoint genes contribute to mitotic checkpoint defects and aneuploidy in other human cancers. Interestingly, the expression of one such gene (*hsMAD2*) was relatively low in breast cancer cells that exhibited an abnormal mitotic checkpoint[20]. Finally, the purposeful activation of cell-cycle checkpoints by exogenous agents might be used to exploit the differences between normal and tumour cells described here and thus improve the selectivity of chemotherapy[16,21,22].

Note added in proof: A partial cDNA for hBUB1 (AF011387) has been independently identified by F. Pangilinan *et al.*[29]. □

Methods

Cell culture and cell-cycle analysis. The derivation and growth conditions of the colorectal cancer cell lines used in this study have been described[8,23,24]. The ten cell lines studied for mitotic checkpoint status were analysed in detail for karyotype and MMR, as described[8]. The four MIN lines (HCT116, DLD1, RKO, and SW48) were MMR-deficient and diploid whereas the six CIN lines were MMR-proficient and aneuploid, with substantial variability in chromosome number and modal chromosome numbers of 71, 119, 82, 86, 96, and 40 in lines HT29, SW480, V400, V429, Caco2, and SW837, respectively. Primary fibroblasts from normal human skin were obtained from Clonetics and used at third passage, when their doubling time was ~26 h, similar to that of the cancer cell lines. Nocodazole or colcemid was added to the media to final concentrations of 0.2 μg ml^{-1} or 1 μg ml^{-1}, respectively. Cells were harvested at 6-h time intervals thereafter, then fixed with glutaraldehyde and stained with Hoechst 33258 (H33258). Viable cells were defined as those without fragmented nuclei or other signs of apoptosis. Flow cytometry (>10,000 cells per sample) was used to evaluate the cell-cycle profile and fluorescence microscopy was used to assess the mitotic index (percentage of viable cells arrested in mitotis). In some experiments, BrdU (10 μM) was added to the cells 2.5 h before harvest and BrdU incorporation was evaluated using a monoclonal antibody to BrdU (Boehringer) and a rhodamine-coupled goat anti-mouse secondary antibody (Pierce).

Cloning of *hBUB1* and *hBUBR1*. Full-length protein and nucleotide sequences of *S. cerevisiae* and murine *BUB1* genes were used to search the National Center for Biotechnology Information expressed sequence tag database (dbEST). Multiple overlapping EST clones were identified for the carboxy-terminal ends of the proteins. To derive the remainder of the sequences, rapid amplification of cDNA ends (RACE) was performed using colonic adenocarcinoma RACE-ready cDNA (Clontech). RT-PCR amplification and sequencing from multiple cDNA samples derived from human tissues provided corrections to the contig

assembled from the databases and EST clones. Genomic clones of each gene were identified by PCR-based screening of a human BAC library (Release III, Research Genetics). FISH was performed on human prometaphase spreads as described[25].

Mutational analysis. CIN status of evaluated lines was documented by the presence of aneuploidy or the absence of MIN[8,26]. Two lines (LoVo and V1394) showed both CIN and MIN, a phenomenon noted previously[8]. Total RNA was purified and used for DNA synthesis with random hexamers and Superscript II (Life Technologies) as described[27]. The following primers were used to amplify *hBUB1* in three overlapping segments: 5′-CATGGACACCCCGGAAAATGTC-3′ and 5′-GCATCTTTGCTGGCCACTGC-3′ for codons 1–404; 5′-GTGGAGACATCCCATGAGGATC-3′ and 5′-GGATCTTCTGCAATGGCAGCG-3′ for codons 304–710; and 5′-AGCCCAAAACAGGCCTTGTCG-3′ and 5′-CAGTGTGATTTTTAAGGACTGTC-3′ for codons 661–1085. The following primers were used to amplify *hBUBR1* in three overlapping segments: 5′-TGTAGCTCCGAGGGCAGG-3′ and 5′-TTGAGAGCACCTCCTACACG-3′ for codons 1–249; 5′-GAGTCTTCTGTACCACAACG-3′ and 5′-AAAACGGAGCTGCTTCTGGC-3′ for codons 218–617; 5′-TCACAGGCTTCAGAAATGTAAC-3′ and 5′-ATACATGGTGATCATAAGAGAAC-3′ for codons 594–1050. The RT-PCR products were purified on an agarose gel and sequenced with a series of internal primers using Thermosequenase (Amersham). The intron–exon structures of selected regions of *hBUB1* and *hBUBR1* were determined through sequence analysis of PCR products generated from genomic DNA. Genomic PCR was performed using primers derived from sequences surrounding the mutations described in the text. DNA from paraffin blocks of the primary tumours from which these lines were derived was purified as described[28]. The sequences of all primers used for mutational analysis are available from the authors upon request.

***hBUB1* expression vectors.** Expression vector pBI-GFP was constructed by insertion of the blunt-ended *Hin*dIII/*Not*I fragment of phGFP-S65T (Clontech) into the *Eco*RV site of pBI (Clontech). pBI-GFP-Bub1WT was constructed by cloning RT-PCR products representing the WT *hBUB1* sequence into the *Not*I and *Sal*I sites of pBI-GFP. pBI-GFP-Bub1*V400 and pBI-GFP-Bub1*V429 were similarly constructed by insertion of RT-PCR products from tumour lines V400 and V429, respectively, into pBI-GFP. HCT116 or DLD1 cells were cotransfected with vector DNA and DNA from a plasmid driving the expression of the tTA transcriptional activator (Clontech) and Lipofectamine Plus (Life Technologies). Twelve hours after transfection, cells were treated with 0.2 μg ml^{-1} nocodazole. BrdU was added to the media 15.5 h later and the cells were collected 2.5 h after BrdU addition. Successfully transfected cells were isolated by sorting on the basis of GFP fluorescence. Sorted cells were analysed by flow cytometry and fluorescence microscopy as described above. BrdU incorporation was compared with that in transfected cells not treated with nocodazole.

Received 7 January; accepted 6 February 1998.

1. Boveri, T. *Zur Frage der Entstehung maligner Tumoren vol. 1* (Gustav Fischer, Jena, 1914).
2. Loeb, L. A. Mutator phenotype may be required for multistage carcinogenesis. *Cancer Res.* **51,** 3075–3079 (1991).
3. Hartwell, L. Defects in a cell cycle checkpoint may be responsible for the genomic instability of cancer cells. *Cell* **71,** 543–546 (1992).
4. Perucho, M. Cancer of the microsatellite mutator phenotype. *Biol. Chem.* **377,** 675–684 (1996).
5. Modrich, P. Strand-specific mismatch repair in mammalian cells. *J. Biol. Chem.* **272,** 24727–24730 (1997).
6. Kolodner, R. D. Mismatch repair—mechanisms and relationship to cancer susceptibility. *Trends Biochem. Sci.* **20,** 397–401 (1995).
7. Kinzler, K. W. & Vogelstein, B. Lessons from hereditary colon cancer. *Cell* **87,** 159–170 (1996).
8. Lengauer, C., Kinzler, K. W. & Vogelstein, B. Genetic instability in colorectal cancers. *Nature* **386,** 623–627 (1997).
9. Strand, M., Prolla, T. A., Liskay, R. M. & Petes, T. D. Destabilization of tracts of simple repetitive DNA in yeast by mutations affecting DNA mismatch repair. *Nature* **365,** 274–276 (1993).
10. Murray, A. W. The genetics of cell cycle checkpoints. *Curr. Opin. Genet. Dev.* **5,** 5–11 (1995).
11. Nasmyth, K. At the heart of the budding yeast cell cycle. *Trends Genet.* **12,** 405–412 (1996).
12. Paulovich, A. G., Toczyski, D. P. & Hartwell, L. H. When checkpoints fail. *Cell* **88,** 315–321 (1997).
13. Nicklas, R. B. How cells get the right chromosomes. *Science* **275,** 632–637 (1997).
14. Li, R. & Murray, A. W. Feedback control of mitosis in budding yeast. *Cell* **66,** 519–531 (1991).
15. Roberts, B. T., Farr, K. A. & Hoyt, M. A. The *Saccharomyces cerevisiae* checkpoint gene BUB1 encodes a novel protein kinase. *Mol. Cell Biol.* **14,** 8282–8291 (1994).
16. Hardwick, K. G., Weiss, E., Luca, F. C., Winey, M. & Murray, A. W. Activation of the budding yeast spindle assembly checkpoint without mitotic spindle disruption. *Science* **273,** 953–956 (1996).
17. Pangilinan, F. & Spencer, F. Abnormal kinetochore structure activates the spindle assembly checkpoint in budding yeast. *Mol. Biol. Cell* **7,** 1195–1208 (1996).
18. Taylor, S. S. & McKeon, F. Kinetochore localization of murine Bub1 is required for normal mitotic timing and checkpoint response to spindle damage. *Cell* **89,** 727–735 (1997).
19. Hanks, S. K. & Quinn, A. M. Protein kinase catalytic domain sequence database: identification of conserved features of primary structure and classification of family members. *Methods Enzymol.* **200,** 38–62 (1991).
20. Li, Y. & Benezra, R. Identification of a human mitotic checkpoint gene: hsMAD2. *Science* **274,** 246–248 (1996).
21. Hartwell, L. H., Szankasi, P., Roberts, C. J., Murray, A. W. & Friend, S. H. Integrating genetic approaches into the discovery of anticancer drugs. *Science* **278,** 1064–1068 (1997).
22. Waldman, T., Lengauer, C., Kinzler, K. W. & Vogelstein, B. Uncoupling of S phase and mitosis induced by anticancer agents in cells lacking p21. *Nature* **381,** 713–716 (1996).
23. Polyak, K., Waldman, T., He, T.-C., Kinzler, K. W. & Vogelstein, B. Genetic determinants of p53 induced apoptosis and growth arrest. *Genes Dev.* **10,** 1945–1952 (1996).
24. Liu, B. *et al.* Mismatch repair gene defects in sporadic colorectal cancers with microsatellite instability. *Nature Genet.* **9,** 48–55 (1995).
25. Lengauer, C. *et al.* Large-scale isolation of human 1p36-specific P1 clones and their use for fluorescence *in situ* hybridization. *Genet. Anal. Tech. Appl.* **11,** 140–147 (1994).
26. Parsons, R. *et al.* Microsatellite instability and mutations of the transforming growth factor beta type II receptor gene in colorectal cancer. *Cancer Res.* **55,** 5548–5550 (1995).
27. Riggins, G. J., Kinzler, K. W., Vogelstein, B. & Thiagalingam, S. Frequency of Smad gene mutations in human cancers. *Cancer Res.* **57,** 2578–2580 (1997).
28. Jen, J. *et al.* Allelic loss of chromosome 18q and prognosis in colorectal cancer. *N. Engl. J. Med.* **331,** 213–221 (1994).
29. Pangilinan, F. *et al.* Mammalian BUB1 protein kinases: map positions and *in vivo* expression. *Genomics* **46,** 379–388 (1997).

Acknowledgements. We thank S. Laken for assistance with the microdissection of tumours, J. Flook for assistance with flow cytometry, and T. Henn for assistance with FISH. This work was supported by the Clayton Fund and grants from the NIH. B.V. and S.D.M. are Investigators of the Howard Hughes Medical Institute.

Correspondence and requests for materials should be addressed to C.L. (lengauer@welchlink.welch.jhu.edu). The accession numbers for *hBUB1* and *hBUBR1* are AF046078 and AF046079, respectively.

Role of calcineurin and Mpk1 in regulating the onset of mitosis in budding yeast

Masaki Mizunuma, Dai Hirata, Kohji Miyahara, Eiko Tsuchiya & Tokichi Miyakawa

Department of Molecular Biotechnology, Graduate School of Engineering, Hiroshima University, Higashi-Hiroshima 739, Japan

Signalling via calcium is probably involved in regulating eukaryotic cell proliferation, but details of its mechanism of action are unknown[1,2]. In *Schizosaccharomyces pombe*, the onset of mitosis is determined by activation of a complex of the p34^{cdc2} protein kinase and a cyclin protein that is specific to the G2 phase of the cell cycle. This activation requires dephosphorylation of p34^{cdc2} (ref. 3). Wee1, a tyrosine kinase that inhibits p34^{cdc2} by phosphorylating it, is needed to determine the length of G2 phase. Here we show that calcium-activated pathways in *Saccharomyces cerevisiae* control the onset of mitosis by regulating Swe1, a Wee1 homologue. Zds1 (also known as Oss1 and Hst1) (refs 4–7) is important in repressing the transcription of *SWE1* in G2 phase. In the presence of high calcium levels, cells lacking Zds1 are delayed in entering mitosis. Calcineurin[8–11] and Mpk1 (refs 12, 13) regulate Swe1 activation at the transcriptional and post-translational levels, respectively, and both are required for the calcium-induced delay in G2 phase. These cellular pathways also induce a G2-phase delay in response to hypotonic shock.

A null mutation of the *ZDS1* gene (Δ*zds1*) in the W303 *S. cerevisiae* strain causes no obvious phenotype[4], although a similar mutation (Δ*oss1* = Δ*zds1*) in other strain backgrounds causes a severe delay in passage through G2 and the cells form a highly elongated bud[5]. However, the Δ*zds1* W303 strain did show a growth defect in rich medium (see Methods) supplemented with $CaCl_2$ (50–300 mM) and the cells formed an elongated bud[5] (data not shown). These Ca^{2+}-induced cell abnormalities were apparently similar to those observed with the Δ*oss1* mutant in rich medium without added $CaCl_2$ (ref. 5). Δ*zds1* cells grown in calcium medium were analysed by flow-cytometry analysis (FACS) and staining with 4,6-diamidino-2-phenylindole (DAPI). Most of the elongated cells had one nucleus at the mother/bud neck, which is characteristic of G2 delay (data not shown). FACS analysis showed that the cells had two copies of the DNA, showing that Ca^{2+} causes severe cell-cycle delay in G2 rather than in earlier stages (Fig. 1).